Magnetic dichroism study of the valence-band structure of perpendicularly magnetized Co/Cu(111)

W. Kuch, A. Dittschar, M. Salvietti, M.-T. Lin, M. Zharnikov, and C. M. Schneider
Max-Planck-Institut für Mikrostrukturphysik, Weinberg 2, D-06120 Halle, Germany

J. Camarero, J. J. de Miguel, and R. Miranda
Departamento de Física de la Materia Condensada, Universidad Autónoma de Madrid, E-28049 Madrid, Spain

J. Kirschner
Max-Planck-Institut für Mikrostrukturphysik, Weinberg 2, D-06120 Halle, Germany
(Received 30 May 1997; revised manuscript received 29 July 1997)

The electronic structure of three monolayers (ML) Co on Cu(111), grown with Pb as a surfactant and capped with two ML Cu, was studied using magnetic circular dichroism in valence-band photoemission. The easy axis of magnetization in these films is perpendicular to the surface, allowing an experimental setup of extreme symmetry (photon spin, light incidence, electron emission, and magnetization all aligned and perpendicular to the surface). In such a geometry features observed in magnetic dichroism can be directly related to the symmetry character of the relativistic band structure. Experimental data in the photon energy range of 6–24 eV are presented. The observed magnetic dichroism and its dispersion with photon energy can be explained on the basis of direct transitions in a bulklike band structure of Co. [S0163-1829(98)04109-5]

I. INTRODUCTION

Magnetic dichroism in photoemission is the modification of intensity distribution curves by reversal of the magnetization direction. It is due to the interplay of the spin orbit and exchange coupling in magnetic materials (see, for example, Refs. 1–4). Since this interplay is of basic importance in the relativistic band structure of ferromagnets, magnetic dichroism in valence-band photoemission should be a most appropriate technique for studying the electronic properties of magnetic materials. Its differential nature allows the facile identification of magnetic contributions in a spectrum and makes it superior to conventional photoemission. In contrast to spin-resolved photoemission, which also probes the exchange-split nature of the valence bands, measuring magnetic dichroism has the advantage of relatively short acquisition times, because only photoelectron intensities are recorded. Furthermore, it has been quite recently reported that due to spin-dependent transport the contribution of surface resonances may be strongly overemphasized in spin-resolved photoemission spectra.[5]

For experimental geometries of high symmetry, analytic considerations yield a set of direct relations between the relativistic symmetry character of the valence bands and the observed dichroism.[6] This has been experimentally verified for perpendicularly magnetized Ni films, where the virtue of magnetic circular dichroism in angular distribution (MCDAD) for band structure investigations has been successfully demonstrated.[4] It has been shown that dichroism spectra deliver an impressive amount of information about the details in the exchange and spin-orbit split band structure compared to conventional photoemission. The usefulness of MCDAD for the investigation of magnetic band structures holds in general for all experimental arrangements, although the interpretation in experimental configurations of low symmetry is less obvious, and additional fully relativistic photoemission calculations may be advisory. Setups of extreme symmetry, on the other hand, in which the magnetization is perpendicular to the surface and aligned to the wave vectors of both the photon incidence and the electron emission, are especially convenient to interpret the data in terms of the band symmetry.[4,6] In such a case a maximum number of different relativistic symmetry characters is assigned to the bands, which together with the nonrelativistic dipole selection rules makes it easy to extract the desired information from the spectra. It is thus desirable to seek geometries with such high symmetries.

In Ref. 4 the direct connection between the relativistic band symmetry and MCDAD was demonstrated for a surface with a fourfold symmetry, namely, the fcc (100) surface of Ni films. The comparison of experimental MCDAD spectra with relativistic photoemission calculations corroborated the band structure origin of the dichroism, giving the experimenter an invaluable tool at hand for band structure investigations of ferromagnets.

In this contribution we will test the analytical expressions of Ref. 6 describing the MCDAD for a surface with threefold symmetry and perpendicular magnetization. To do so we use perpendicularly magnetized Co films on Cu(111), grown with Pb as surfactant. The MCDAD will then be applied to study the magnetic band structure of the Co films.

Without surfactants, the growth of Co on Cu(111) is accompanied by three-dimensional island formation and stacking faults.[9–11] At film thicknesses above 3 monolayers (ML) a considerable amount of Co assumes the hcp phase.[9,10,12] A perpendicular easy axis of the magnetization was reported exclusively for very thin film thicknesses.[13,14] Capping the Co film with Cu increases the perpendicular anisotropy[14] and extends this thickness region for the perpendicular magnetization up to 2 ML.[15] Previous spin-resolved measurements

of Co/Cu(111) (Refs. 7,8) were carried out at film thicknesses where the Co films are mainly hcp. Near the Γ point of the Brillouin zone an exchange splitting of 1.4 ± 0.15 eV for the lower d bands was found.[7] Varying the emission angle for photoemission excited by NeI radiation yielded a dispersion predominantly of minority bands.[8]

The morphology of the Co films can be significantly improved by using Pb as a surfactant during the film growth.[16] The Pb is floating on the surface of the Co film and also on top of a Cu cap layer at all stages of deposition.[16] The film growth is forced into a layer-by-layer mode, and the formation of stacking faults is effectively suppressed.[16] The much lower roughness of the Pb-grown films and the absence of stacking faults also affects the magnetic properties: In a capped Cu/Co/Cu(111) structure a perpendicular magnetization is now observed up to a Co thickness of 3–4 ML.[15] This and the observation of a complete antiferromagnetic interlayer exchange coupling in Pb-grown Co/Cu/Co multilayers[15,17] points toward a much smoother Co/Cu interface compared to films grown without a surfactant.

To study the bulk band structure by using thin films it is favorable to go to film thicknesses as high as possible. Usually the magnetic dipole interaction acts to keep the magnetization in the film plane when the thickness is increased. In the Co/Cu(111) system, 3–4 ML seems to be about the highest Co film thickness with an out-of-plane remanent magnetization.[15] We therefore used (Pb)/2 ML Cu/3 ML Co/Cu(111) films for the dichroism measurements. These films offer the advantage of a well-defined fcc structure with a low surface or interface roughness. We will show that the MCDAD of these films exhibits already a distinct dispersion along the Λ axis which can be explained by direct transitions within a bulklike band structure.

II. EXPERIMENT

The experiments were carried out in a UHV chamber (base pressure 1×10^{-8} Pa) equipped with facilities for low-energy electron diffraction (LEED), Auger electron spectroscopy (AES), magneto-optical Kerr-effect (MOKE), medium energy electron diffraction (MEED), and thin film growth. Details of the setup may be found in Ref. 18.

Before deposition of Co and Cu, 1.5 ML of Pb were evaporated onto the clean sample. Pb was evaporated from a stainless steel crucible by indirect heating with a tungsten filament. The Pb coverage was calibrated by monitoring the MEED specular intensity during growth. 1.5 ML of Pb showed the typical (4×4) reconstruction LEED pattern.[15,19] The sample temperature was 450 K during Pb evaporation, which is still below the temperature at which embedded Pb atoms on Cu(111) have been found,[19] and 300 K for the subsequent Co and Cu depositions. High purity Co and Cu was evaporated by electron bombardment from a cobalt rod and a molybdenum crucible, respectively. Typical deposition rates for all three materials were 0.2 ML/min, while the overall pressure in the chamber did not exceed 2×10^{-8} Pa (5×10^{-8} Pa in the case of Pb). No surface contamination above the AES detection limit ($\approx 1\%$) could be detected after any of the deposition steps. It was checked using AES that the complete Pb coverage was floating on the surface after deposition of the Co or Cu films. Identical Pb (4×4) LEED patterns were observed before and after Co and Cu deposition. All of the 2 ML Cu/3 ML Co/Cu(111) films produced rectangular hysteresis loops of the polar Kerr effect at room temperature.

Photoemission spectra were taken at the 6.5 m normal-incidence monochromator beamline of the Berlin synchrotron radiation facility (BESSY), with a circular polarization of about 90%.[20] As mentioned in Sec. I, the spectra presented in this paper were taken in the totally symmetric configuration, i. e., normal incidence of the incoming radiation, and normal emission of the outgoing photoelectrons. The sample temperature during the acquisition of the photoemission spectra was 300 K. The presence of the remanent magnetization was checked by MOKE before and after each of the measurements. To rule out apparatus induced asymmetries, spectra for both helicities of the incoming light were taken for both magnetization directions of the sample.

The electron spectrometer is described in detail elsewhere.[21] It allows the detection of normally emitted electrons for normal incidence of the incoming radiation. For the measurements presented in this paper it was operated at a fixed pass energy of 8 eV, resulting in an overall energy resolution of approximately 200 meV (including the monochromator resolution). The angular acceptance can be estimated to be less than $\pm 2°$.

III. THEORY

Before turning to the experimental results and their interpretation, it is useful to recall briefly the analytical description of MCDAD by J. Henk *et al.*[6] Instead of using the nomenclature of the magnetic double group, we follow the concept of Ref. 6 and express initial and final states in terms of the symmetries of the nonmagnetic double group, but with Kramer's degeneracy lifted.

In the nonmagnetic case, the symmetry of the (111) surface is C_{3v}. Relativistic electronic states can be classified by two irreducible representations of the double group Λ_6 and $\Lambda_{4,5}$. The final states for normal emission have Λ_6 symmetry. For normal light incidence and normal electron emission, only transitions between initial states containing Λ^3 spatial symmetry and final states with Λ^1 spatial symmetry are allowed. Although the spatial symmetry, i.e., the irreducible representation of the (nonrelativistic) single group, is not a good quantum number in the presence of spin-orbit coupling, we will append an upper index to the double group representation indicating the predominant spatial symmetry.

The presence of the perpendicular magnetization reduces the symmetry of the system and lifts Kramer's degeneracy. Each of the two-dimensional irreducible double group representations Λ_6 and $\Lambda_{4,5}$ of the nonmagnetic case decompose into a pair of one-dimensional representations, labeled according to Ref. 6 Λ_6+, Λ_6-, $\Lambda_{4,5}+$, and $\Lambda_{4,5}-$. The $+$ $(-)$ sign thereby denotes the symmetry behavior under time reversal. It does not refer to majority or minority spin, because the latter is, as the spatial symmetry, not a good quantum number in the presence of spin-orbit coupling. Without interband hybridization, however, bands with opposite spin character exhibit also opposite time-reversal symmetry, in the sense that majority bands with Λ^3 spatial symmetry have negative $(-)$ time-reversal symmetry.

Transitions in the totally symmetric experimental configuration occur, in our nomenclature, between initial states of Λ_6^3+, Λ_6^3-, $\Lambda_{4,5}^3+$, and $\Lambda_{4,5}^3-$ symmetry, and final states of Λ_6^1+ and Λ_6^1- symmetry. The contributions of these transitions to the photoemission intensity for parallel or antiparallel alignment of photon spin σ and sample magnetization $\mathbf{M}$ can be expressed in terms of partial matrix elements $M_i^{ss'}$. Here, the notation is that $M_{4,5}^{+-}$, for example, describes transitions from an initial state with $\Lambda_{4,5}^3-$ symmetry to a final state with Λ_6^1+ symmetry. The photoemission intensity for parallel alignment of σ and $\mathbf{M}$, according to Ref. 6, is

$$I(\uparrow\uparrow)=2|M_6^{+-}|^2+|M_{4,5}^{-+}|^2+|M_{4,5}^{--}|^2. \tag{1}$$

For antiparallel alignment, we obtain

$$I(\uparrow\downarrow)=2|M_6^{-+}|^2+|M_{4,5}^{+-}|^2+|M_{4,5}^{++}|^2. \tag{2}$$

In the nonrelativistic limit there are two majority and two minority bands with Λ^3 spatial symmetry along the Λ axis of the Brillouin zone. Each of these four bands is energetically split by the spin-orbit interaction into two bands with $\Lambda_{4,5}$ and Λ_6 symmetry. Because the spin-orbit coupling in the $3d$ valence bands of Co is about one order of magnitude smaller than the exchange splitting, we end up with closely spaced doublets of bands with parallel spin and different double group symmetry, separated from other doublets with opposite spin by the exchange splitting. This is true as long as no hybridization with other bands occurs.

Let us now consider the dichroism one should observe by changing either the light helicity or the magnetization direction. The dichroism is the intensity difference upon helicity or magnetization reversal:

$$D=I(\uparrow\uparrow)-I(\uparrow\downarrow). \tag{3}$$

The contribution of the Λ_6 bands to the dichroism D is of the type $|M_6^{+-}|^2-|M_6^{-+}|^2$. This means, for a given light helicity only bands with either Λ_6+ symmetry *or* with Λ_6- symmetry contribute to the spectra. Without hybridization, these bands are separated by the exchange splitting; this situation should lead to a pronounced dichroism. Bands with $\Lambda_{4,5}$ symmetry, on the other hand, give a contribution $|M_{4,5}^{-+}|^2-|M_{4,5}^{++}|^2+|M_{4,5}^{--}|^2-|M_{4,5}^{+-}|^2$. Here, contrary to the Λ_6 bands, transitions from both $\Lambda_{4,5}+$ *and* $\Lambda_{4,5}-$ bands occur for each light helicity. Changing the helicity, transitions from the same initial state bands, but into different final state bands are excited. The dichroism in $\Lambda_{4,5}$ related transitions thus depends on the exchange splitting between the Λ_6^1+ and Λ_6^1- final state bands, which in general will be much smaller than in the initial state. Only for a nonvanishing exchange splitting in the upper bands do transitions into the two exchange-split final state bands take place at a slightly different value of the electron wave vector component perpendicular to the surface $k_\perp$. This will lead to a dichroism, but only if there is a sizeable dispersion of the lower bands. For either a vanishing exchange splitting of the final state bands or a vanishing dispersion of the initial state bands there will be no dichroism. We therefore expect that the contribution of the $\Lambda_{4,5}$ bands to the total dichroism will be very small compared to that of the Λ_6 bands. In addition, it should decrease towards higher photon energies, because the exchange splitting of the final state bands decreases with distance to the Fermi level. Considering the small energetic separation between two spin-orbit split bands of $\Lambda_{4,5}$ and Λ_6 symmetry,[22] the dichroism of the former will probably not be observed in the experiment. The main dichroism will arise from transitions involving Λ_6 initial state bands only. This is schematically illustrated in Fig. 1. In the bottom panel the energetic positions of four bands with Λ_6^3+, Λ_6^3-, $\Lambda_{4,5}^3+$, and $\Lambda_{4,5}^3-$ symmetry in the absence of hybridization are marked by vertical lines. The influence of the spin-orbit splitting is indicated by small arrows. In the case of vanishing final state exchange splitting, for parallel or antiparallel alignment of photon spin σ and magnetization $\mathbf{M}$, either the Λ_6^3+ or the Λ_6^3- bands, respectively, do not contribute to the photoemission spectrum. In the center panel of Fig. 1, schematic intensity distribution curves for the two cases [σ and $\mathbf{M}$ parallel $I(\uparrow\uparrow)$: solid line and σ and $\mathbf{M}$ antiparallel $I(\uparrow\downarrow)$: dotted line] are shown. The difference between both is displayed in the top panel. It exhibits plus and minus peaks at the energetic positions of Λ_6^3- and Λ_6^3+ bands, respectively.

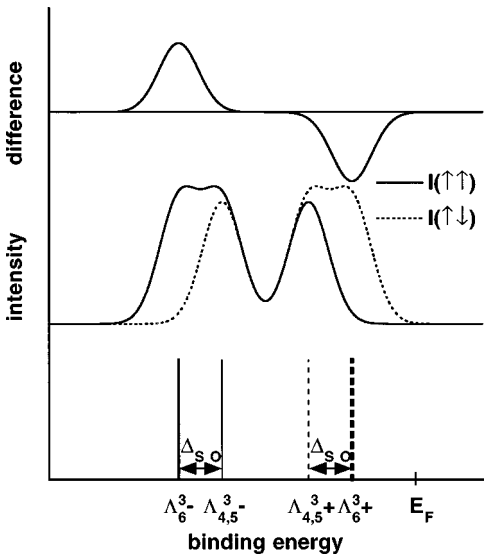

FIG. 1. Bottom: schematic representation of four bands of Λ_6^3-, $\Lambda_{4,5}^3-$, $\Lambda_{4,5}^3+$, and Λ_6^3+ symmetry contributing to the spectra in the totally symmetric geometry. The arrows indicate the splitting due to spin-orbit interaction. Center: schematic intensity distribution curves for parallel (solid line) and antiparallel alignment (dotted line) of photon spin and magnetization direction. Top: intensity difference of the spectra of the center panel. Plus and minus peaks are located at the energetic positions of Λ_6^3- and Λ_6^3+ bands.

The situation is summarized as follows: without hybridization between different bands, one of the two bands of a spin-orbit split majority (minority) doublet will give rise to a positive (negative) asymmetry. This intensity asymmetry is correlated to the symmetry character of the bands, and reflects directly the spin polarization in the absence of interband hybridization. Note that if the spin-orbit interaction is small compared to the width of the peaks, measuring the dichroic difference will yield information equivalent to explicitly measuring the spin polarization.

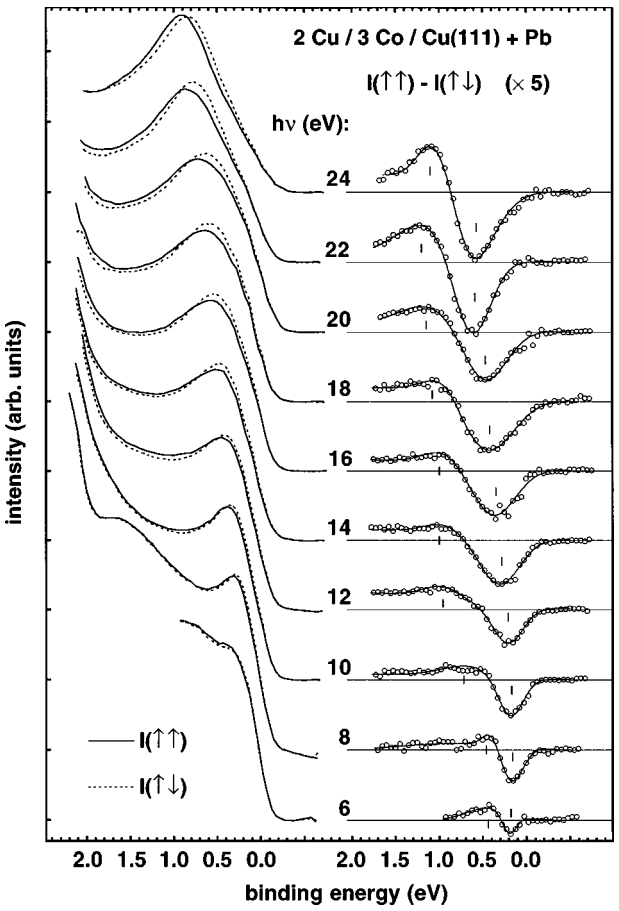

FIG. 2. Left: Series of partial intensity spectra of 2 ML Cu/3 ML Co/Cu(111), grown with Pb as a surfactant, for different photon energies $h\nu$. Shown are spectra for parallel (solid lines) and antiparallel alignment (dotted lines) of photon spin and magnetization direction. Right: differences between the partial spectra of the left-hand side, scaled by a factor of 5 (circles). The solid lines are smoothing splines to the data. The small vertical bars mark peak positions of plus and minus peaks.

IV. RESULTS

Figure 2 shows the results of the MCDAD measurements. On the left-hand side photoemission intensity curves at different photon energies for parallel [$I(\uparrow\uparrow)$, solid lines] and antiparallel alignment of photon spin and sample magnetization [$I(\uparrow\downarrow)$, dashed lines] are depicted. At 6 eV photon energy a small peak at 0.3 eV binding energy is observed, superimposed on a large secondary electron background. It becomes more pronounced at $h\nu=8$ eV, and disperses towards higher binding energies with increasing photon energy. This peak is attributed to emission from Co $3d$ states. The contribution of the Cu $3d$ states to the spectra is expected at binding energies of 2 eV and higher.[23,24] The increase in intensity at the end of each spectrum marks indeed the shoulder of an intense Cu $3d$ peak, which shows a similar dispersion with photon energy as does the Co peak.

The $I(\uparrow\uparrow)$ and $I(\uparrow\downarrow)$ spectra exhibit clear differences, which means that there is a pronounced magnetic dichroism. Conventional photoemission, at that point, would deliver only the summed average of both curves. From that alone, it would be very hard to extract more information than just the general dispersion behavior, because any decomposition of the peaks would require knowledge of the partial photoemission cross sections and the hole-lifetime broadening of the close-lying bands. The differential nature of MCDAD, however, allows the precise separation of bands with different double-group symmetry. To illustrate this, the differences between the spectra of parallel and antiparallel alignment of σ and **M** from the left-hand side of Fig. 2 are depicted on the right-hand side, magnified in intensity by an (arbitrary) factor of 5. Circles represent the experimental data and solid lines are the result of smoothing splines. At 6 eV photon energy, a small but distinct plus-minus feature is made out at binding energies of 0.2 and 0.4 eV for the minus and plus peaks, respectively. Both peaks shift towards higher binding energy with increasing photon energy. The amplitude of the minus peak thereby increases, whereas the plus peak is getting broader and less defined at photon energies between 10 and 20 eV. Possible reasons for this broadening of the difference peaks will be discussed in Sec. V. At $h\nu=24$ eV, both peaks are again very pronounced and well defined, with binding energies of 0.6 and 1.1 eV, respectively. At this photon energy, the peak maxima reach values of -5.8 and 2.5 % of the summed photoemission intensity $I(\uparrow\uparrow)+I(\uparrow\downarrow)$.

We now turn back to the analytical considerations of Sec. III. As discussed there, only the first terms of Eqs. (1) and (2) should give sizeable contributions to the dichroism. Bands of Λ_6^3+ symmetry [first term of Eq. (2)] give a negative contribution to the difference $I(\uparrow\uparrow)-I(\uparrow\downarrow)$ and bands of Λ_6^3- symmetry [first term of Eq. (1)] a positive one. We therefore correlate the negative peak at lower binding energies to a Λ_6^3+ band, and the positive peak at higher binding energies to a Λ_6^3- band. As already mentioned, without spin-orbit hybridization Λ_6^3+ means minority spin, and Λ_6^3- majority spin.

The peak positions of the two peaks in the difference spectra of Fig. 2 are traced by small vertical bars, and the corresponding binding energies plotted in Fig. 3 as solid triangles versus the perpendicular component of the wave vector $k_\perp$. The latter was obtained by assuming a simple free-electron-like final state dispersion with an inner potential of 10 eV. The error bars reflect the accuracy with which the energetic positions of the respective difference peaks can be determined. Up (down) triangles correspond to the peak positions of the plus (minus) peaks. They are connected in Fig. 3 by solid (broken) lines, which serve as a guide to the eye. At higher photon energies, the transitions take place at lower k values, i. e., nearer to the Γ point of the Brillouin zone.

Also shown in the inset of Fig. 3 is a fully relativistic calculation of Ebert of the Co bulk band structure along the Λ axis and for an in-plane magnetization along the [110] azimuth.[25] Bands with predominant minority spin character are depicted as dotted lines, and bands with predominant majority character as solid lines. Although the calculation was done for an in-plane magnetization, we will label the bands as in the case of perpendicular magnetization. The different symmetry of the in-plane and perpendicularly magnetized system affects mainly the crossings between bands, and to a lesser amount the energetic positions of the individual bands. Bands which have (in the case of perpendicular magnetization) Λ_6 double group symmetry and a predomi-

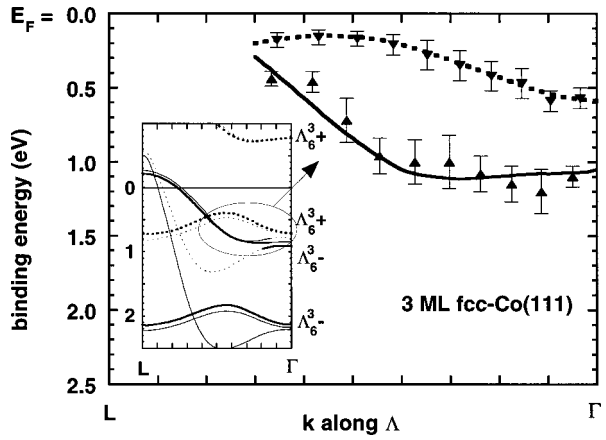

FIG. 3. Plot of the peak positions of the difference spectra from Fig. 2 as a function of electron wave vector perpendicular to the surface. Up (down) triangles denote positions of plus (minus) peaks of the difference spectra. k values were obtained by assuming free-electron-like final states with an inner potential of 10 eV. Lines are guides to the eye. The inset shows a fully relativistic band structure calculation of Ebert (Ref. 25) (see text). Bands with predominant majority (minority) spin character are depicted as solid (dotted) lines. Thick lines denote bands with Λ_6^3 symmetry, which are responsible for the dichroism. Only these bands are mapped by MCDAD. The region probed by our experiment is indicated by an ellipse.

nant Λ^3 spatial symmetry character, i.e., Λ_6^3 in our nomenclature, are emphasized by thick (dotted or solid) lines. As outlined before, these bands are mainly responsible for the magnetic dichroism. The spin-orbit coupling lifts the energetic degeneration of the two-dimensional Λ^3 bands; this is seen as splitting of Λ^3 bands of the nonrelativistic case into two close-lying bands of Λ_6 and $\Lambda_{4,5}$ double group symmetry, separated by the spin-orbit interaction, which in the valence bands of the $3d$ transition metals is of the order of 100 meV.[22]

A region of spin-orbit induced hybridization as a consequence of avoided crossings between bands of identical double group symmetry is present at about 15% $\overline{\Gamma L}$. At this position, the spin character as well as the spatial symmetry are gradually exchanged between two bands of Λ_6- symmetry. This can be followed as the band depicted by a thick solid line (Λ_6^3-) turns into a thin dotted line (Λ_6^1-).

V. DISCUSSION

Comparing the experimentally observed dispersion of the plus and minus peaks of the asymmetry spectra (Fig. 3) with the calculated bulk band structure (inset of Fig. 3), the band structure origin of the magnetic circular dichroism becomes immediately obvious. The dispersion of the minus peaks of the difference spectra with decreasing photon energy displays directly the dispersion of the lower minority band (Λ_6^3+) with increasing $k_\perp$ away from the Γ point. The plus peaks follow the dispersion of the lower majority band (Λ_6^3-), with little dispersion near Γ, and an increasing upwards dispersion when going from Γ to L. The experimental dispersion of the dichroic features is hence consistent with the bulk band dispersion of fcc Co along the Λ axis. No features are observed indicating a band structure related to hcp Co characterized by its reduced Brillouin zone and the doubled number of bands.[8]

As mentioned in the previous section, the plus peaks in the difference spectra at photon energies between 10 and 20 eV are rather broad and less pronounced compared to those at photon energies below 10 or above 20 eV. One reason for this observation could be the above mentioned hybridization between bands of Λ_6- double group symmetry, and the consequent simultaneous presence of two bands containing Λ_6^3- symmetry (cf. Fig. 3, inset). In the hybridization region, the parabola shaped sp-like band contains a mixture of Λ^3 and Λ^1 spatial symmetry (and hence also a mixture of spin-up and spin-down character). It is conceivable that not only in the vicinity of the Γ point but also further away there is still a considerable portion of Λ_6^3- symmetry in that band. This would contribute a positive signal at the binding energy of that band to the dichroism, and could be a reason for the broad plus feature which is observed between 10 and 20 eV photon energy (Fig. 2). At higher photon energies the transitions occur nearer to the Γ point where these two bands are closer in energy, whereas at lower photon energies regions in k space are probed which are further away from the hybridization region. Both could account for the narrower peaks at these photon energies.

Another possible explanation for the broadening could be the influence of the lower majority band around 2 eV binding energy, which exhibits the same double group symmetry, and should hence contribute with the same (positive) sign to the magnetic dichroism as the higher majority band. A smearing out of two plus peaks could as well give rise to the observed broad plus feature. The energetic separation of the two majority bands is larger for the two highest and the two lowest photon energies, which would explain the better defined plus peaks observed there.

The emission from the lower majority band is, however, not well resolved in the photoemission intensity curves (left-hand side of Fig. 2). This may be due to a strongly enhanced lifetime broadening at higher binding energies. Such a strong broadening of peaks at higher binding energy is not unusual for photoemission from thin film systems.[5] The peak in the spectrum of $h\nu=8$ eV around 1.6 eV binding energy, and some of the intensity between the Co peak near the Fermi edge and the Cu $3d$ peak for photon energies up to 20 eV may be assigned to emission from that band. At higher binding energies, as seen from Fig. 2, it is difficult to analyze the magnetic dichroism because of spin-dependent scattering of spin-polarized substrate photoelectrons in the magnetic layer. This spin-filter effect itself also generates a prominent ''magnetic dichroism.''[24] It should not be confused with the effect of spin-dependent transport of the photoelectrons from the magnetic film itself mentioned in Sec. I, which may hamper the analysis of spin-resolved measurements,[5] because the latter effect has no influence on MCDAD. Whereas the former only exists in films thin enough to permit the detection of substrate or seed layer photoelectrons, the latter is present also in bulk samples. The immunity of MCDAD with respect to spin-dependent transport of the photoelectrons after excitation must be counted as an advantage over spin-resolved photoemission.

Although the qualitative agreement between the calcu-

lated band structure and the experimentally observed dispersion of the dichroism features is very good, and clearly proves the interpretation in terms of relativistic band symmetries as outlined in Sec. III, the exact energetic positions and the dispersion of the bands differ. The main discrepancy between experiment and theory concerns the energetic separation between the upper and lower *d* bands. In the experiment, the upper majority and the lower minority band are sampled. Near Γ we find binding energies for these bands of 1.1 ± 0.1 and 0.6 ± 0.1 eV, respectively. This is in good agreement with spin-resolved measurements of Co/Cu(111) films at higher thicknesses, in which values of 1 and 0.7 eV were obtained,[7] although the separation between the bands is somewhat smaller than in our experiment. One has to keep in mind, however, that we are probing the binding energies of only one of each of the spin-orbit split pairs of bands, whereas spin-resolved photoemission determines the center of both. This should yield a difference in the band separation of the size of the spin-orbit splitting.[22] From the band structure calculation, binding energies of 0.9 and 0.7 eV are found at Γ for the positions of the Λ_6^3- and Λ_6^3+ bands, respectively. The top of the Λ_6^3+ band, as found from our dichroism measurements, is located at a binding energy of 0.15 ± 0.05 eV. In the calculation, it only reaches up to 0.4 eV below E_F. As a consequence of the larger band separation in the experimental data, the crossing point between the two bands, in the calculation around 55% $\overline{\Gamma L}$, is located at higher *k* values in the experiment. At 65% $\overline{\Gamma L}$, the highest *k* value accessible to our range of photon energies, they are still separated.

In general the electronic properties of a 3 ML Co film may very well deviate from bulk properties and lead to different binding energies of the states. We therefore consider the observed band dispersion as an experimental result, which reflects the band structure of a 3 ML Co film, grown with Pb as surfactant and sandwiched between Cu. Besides the influence of the finite thickness, another reason for the quantitative discrepancy between experiment and theory could be that the exchange splitting of the upper bands is somehow overestimated in the band structure calculation. Whereas the exchange splitting of the lower bands, 1.4 eV, is identical to the one found with spin-resolved photoemission, the exchange splitting of the upper bands is higher than experimentally observed. Combining inverse photoemission data of Ref. 26 with the spin-resolved photoemission data of Ref. 7 results in an exchange splitting for the upper bands of 1.15 ± 0.15 eV.[7] In the calculation, the average splitting is 1.6 eV. This may be a hint towards the influence of many-body effects on the photoemission spectra similar to the case of Ni. It was already pointed out theoretically[27] and shown experimentally[28] that the influence of many-body effects may also be important in photoemission from Co ultrathin films.

Another aspect of the present result is that in films as thin as 3 ML there is already a bulklike band structure with a pronounced dispersion, which in our case is even slightly stronger than in the corresponding bulk band structure calculation. On the first look it may be astonishing that in a film consisting of only three atomic layers there should be such a strong dispersion; one would expect a strongly reduced band width due to the reduced coordination of the surface and interface atoms and the two-dimensional character of the film. None of this is observed. Spin-resolved photoemission of Co/Cu(111) revealed a bulklike behavior of Co 3*d* states already at coverages as low as 2 ML.[7] In a recent study Mankey *et al.* showed that angular distributions of photoelectrons of Ni/Cu(001) exhibited bulklike electronic dispersion even in films as thin as 1.2 ML.[29] This is attributed to hybridization of the electronic states with the substrate. For a small lattice mismatch between substrate and film, such a hybridization imposes the Bloch periodicity of the substrate on the electronic wave functions in the film. We suggest that in our Co/Cu(111) films a similar hybridization between Co and Cu states is also the origin of the strong $k_\perp$ dispersion. As in the ultrathin Ni films[29] no narrowing of the *d* bands with respect to the bulk band structure is observed. The electronic structure of Co and Cu is very similar, differing primarily in band fitting, and the lattice mismatch is only 1.8%. This favors the hybridization of certain substrate and film states, which leads to the development of the characteristics of a bulk electronic structure in the ultrathin film.

VI. CONCLUSION

A magnetic dichroism study of the electronic properties of epitaxial Co/Cu(111), grown with Pb as a surfactant, was performed. The experimental dispersion of dichroism peaks and its coincidence with expected band dispersions from band structure calculations leads to several conclusions. First, the theoretical description of the dichroism in terms of direct transitions between valence bands of different double group symmetries, as outlined in Sec. III, is appropriate for the conclusive and consistent interpretation of all of the experimental MCDAD data. The analytical expressions of Ref. 6 link peaks in the difference spectra to the symmetry of valence bands. This was experimentally verified also for the threefold surface of Co/Cu(111), where the content of information of intensity spectra for opposite orientation of light helicity and magnetization direction is comparable to explicitly spin-resolved photoemission measurements. Second, by varying the photon energy the dispersion of the participating bands could be mapped. In 3 ML perpendicularly magnetized Co(111) films the observed dichroism yields the dispersion of bulklike bands. No band narrowing with respect to bulk band structure calculations is found. This is attributed to hybridization with the substrate periodic electronic states. Third, the experimentally observed band structure points towards an fcc structure of the Co film. No indications for the presence of hcp Co were found. Fourth, the relative energetic position of the upper majority and lower minority *d* band is slightly different with respect to band structure calculations[25] and previously published photoemission data.[7] The higher separation at the Γ point between these two bands found here may be a hint towards the influence of many body effects. Altogether, the present work demonstrates the capability of magnetic circular dichroism in valence-band photoemission for electronic band structure investigations of magnetic thin films. The differential nature of the effect makes it insensitive to contributions of nonmagnetic overlayers, which should in principle also allow for the study of buried magnetic layers, e.g., in devices or multilayered stacks.

ACKNOWLEDGMENTS

We would like to thank B. Zada for her expert technical support, and the BESSY staff for general support during beam time. Funding by the German minister of education, science, research, and technology (BMBF) under Contract No. 05 621EFA 0 is gratefully acknowledged. The exchange of researchers was financed by Spain-Germany Acción Integrada No. AI 96-19. M. S. thanks the Alexander von Humboldt-Stiftung, and M. Z. the Max-Planck-Gesellschaft for financial support.

[1] L. Baumgarten, C. M. Schneider, H. Petersen, F. Schäfers, and J. Kirschner, Phys. Rev. Lett. **65**, 492 (1990).
[2] B. T. Thole and G. van der Laan, Phys. Rev. B **44**, 12 424 (1991).
[3] T. Scheunemann, S. V. Halilov, J. Henk, and R. Feder, Solid State Commun. **91**, 487 (1994); J. Henk, S. V. Halilov, T. Scheunemann, and R. Feder, Phys. Rev. B **50**, 8130 (1994).
[4] W. Kuch, A. Dittschar, K. Meinel, M. Zharnikov, C. M. Schneider, J. Kirschner, J. Henk, and R. Feder, Phys. Rev. B **53**, 11 621 (1996); W. Kuch, M. Zharnikov, A. Dittschar, K. Meinel, C. M. Schneider, J. Kirschner, J. Henk, and R. Feder, J. Appl. Phys. **79**, 6426 (1996).
[5] A. Fanelsa, E. Kisker, J. Henk, and R. Feder, Phys. Rev. B **54**, 2922 (1996).
[6] J. Henk, J. Scheunemann, S. V. Halilov, and R. Feder, J. Phys.: Condens. Matter **8**, 47 (1996).
[7] U. Alkemper, C. Carbone, E. Vescovo, W. Eberhardt, O. Rader, and W. Gudat, Phys. Rev. B **50**, 17 496 (1994).
[8] M. Getzlaff, J. Bansmann, J. Braun, and G. Schönhense, J. Magn. Magn. Mater. **161**, 70 (1996).
[9] J. de la Figuera, J. E. Prieto, C. Ocal, and R. Miranda, Phys. Rev. B **47**, 13 043 (1993).
[10] M. T. Kief and W. F. Egelhoff, Jr., Phys. Rev. B **47**, 10 785 (1993).
[11] R. Miranda, Phys. Scr. **T49**, 579 (1993).
[12] V. Scheuch, K. Potthast, B. Voigtländer, and H. P. Bonzel, Surf. Sci. **318**, 115 (1994); P. Le Fevre, H. Magnan, O. Heckmann, V. Briois, and D. Chandesris, Phys. Rev. B **52**, 11 462 (1995).
[13] M. T. Kief and W. F. Egelhoff, Jr., J. Appl. Phys. **73**, 6195 (1993).
[14] F. Huang, M. T. Kief, G. J. Mankey, and R. F. Willis, Phys. Rev. B **49**, 3962 (1994).
[15] J. Camarero, T. Graf, J. J. de Miguel, R. Miranda, W. Kuch, M. Zharnikov, A. Dittschar, C. M. Schneider, and J. Kirschner, Phys. Rev. Lett. **76**, 4428 (1996).
[16] J. Camarero, L. Spendeler, G. Schmidt, K. Heinz, J. J. de Miguel, and R. Miranda, Phys. Rev. Lett. **73**, 2448 (1994).
[17] W. Kuch, A. Dittschar, M.-T. Lin, M. Salvietti, M. Zharnikov, C. M. Schneider, J. Kirschner, J. Camarero, J. J. de Miguel, and R. Miranda, J. Magn. Magn. Mater. **170**, L13 (1997).
[18] F. Baudelet, M.-T. Lin, W. Kuch, K. Meinel, B. Choi, C. M. Schneider, and J. Kirschner, Phys. Rev. B **51**, 12 563 (1995).
[19] C. Nagl, O. Haller, E. Platzgummer, M. Schmid, and P. Varga, Surf. Sci. **321**, 237 (1994).
[20] F. Schäfers, W. Peatman, A. Eyers, C. Heckenkamp, G. Schönhense, and U. Heinzmann, Rev. Sci. Instrum. **57**, 1032 (1986).
[21] C. M. Schneider, J. J. de Miguel, P. Bressler, P. Schuster, R. Miranda, and J. Kirschner, J. Electron Spectrosc. Relat. Phenom. **51**, 263 (1990).
[22] Experimental values for the spin-orbit splitting of the 3*d* valence bands of Cu and Ni, for example, are 150 meV (Refs. 21,24) and 50 meV (Ref. 4), respectively.
[23] H. Eckardt, L. Fritsche, and J. Noffke, J. Phys. F **14**, 97 (1984).
[24] W. Kuch, M.-T. Lin, K. Meinel, C. M. Schneider, J. Noffke, and J. Kirschner, Phys. Rev. B **51**, 12 627 (1995).
[25] H. Ebert (private communication).
[26] G. J. Mankey, R. F. Willis, and F. J. Himpsel, Phys. Rev. B **47**, 190 (1993).
[27] C. Chen, Phys. Rev. Lett. **64**, 2176 (1990); Phys. Rev. B **48**, 1318 (1993).
[28] C. M. Schneider, U. Pracht, W. Kuch, A. Chassé, and J. Kirschner, Phys. Rev. B **54**, R15 618 (1996).
[29] G. J. Mankey, K. Subramanian, R. L. Stockbauer, and R. L. Kurtz, Phys. Rev. Lett. **78**, 1146 (1997).